Structures of Monodisperse Nylon 6 Oligoamides. Onset of Chain-folding

Sharon J. Cooper, Edward D. T. Atkins,* and Mary J. Hill

H.H.Wills Physics Laboratory University of Bristol, Tyndall Avenue, Bristol BS8 1TL, U.K.

Received April 2, 1998; Revised Manuscript Received May 29, 1998

ABSTRACT: Crystals were grown of the 5-amide, 9-amide, and 17-amide nylon 6 monodisperse oligoamides and investigated using electron microscopy (real space and diffraction) and X-ray diffraction. Analyses of the data allowed us to determine the crystalline structures and relate them to the morphology. Under our crystallization conditions, the 5-amide chains are unfolded and crystallize in the usual nylon 6 α-structure, i.e., an apolar arrangement of chains, directed parallel to the layer normal, within hydrogen-bonded sheets which stack via van der Waals interactions. In chain-folded nylon polymers such as nylon 6, the length of the straight stems is approximately 5 to 7 nm; this is equivalent to about six to eight amide units. Therefore it is not too surprising that the 5-amide molecule, of length 4.6 nm, remains unfolded. If the 9-amide molecules (length 8 nm) fold, we would expect them to create hairpin-like structures with four, or close to four, amide units in adjacent straight stems. Our results show that, depending on the crystallization conditions, both unfolded and once-folded conformations can occur for this 9-amide oligomer. In the unfolded conformation, the straight-stem chains crystallize in the nylon 6 γ-phase structure as opposed to the usual α-phase structure. The once-folded structure for the 9-amide chain represents the *onset of folding* in these nylon 6 monodisperse oligoamides and the lamellar stacking periodicity (LSP) is 4.60 nm. This once-folded conformation is similar to the usual nylon 6 α-phase structure. The 17-amide chains crystallize in a twice-folded conformation, also with the nylon 6 α-phase structure, reinforcing the notion that once the chains are long enough to start folding, the pattern of behavior approaches that of the nylon 6 polymer. In this case, the LSP value is 5.36 nm.

Introduction

For some time we have been engaged in studies of solution crystallized lamellae of nylons.[1−9] We have found that there are a small, select number of crystal structures. Consideration of the individual chain stereochemistry, in particular the relative polarity and frequency of the amide units along the chain, the requirements for chain folding, and cooperative hydrogen bonding, lead to rich and subtle variations in the details of the resulting structures (e.g.[7−9]). In collaboration[10] with Drs. G. Brooke and S. Mohammed at the Chemistry Department, University of Durham, we have been able to specify a range of nylon stereochemistries and chain lengths for pedigree monodisperse oligoamides with short alkane chain terminating units.[11,12] We have reported our results on the 3-amide oligomers of both nylon 6 6 and nylon 6.[13] In this contribution, we study the longer 5-, 9-, and 17-amide oligomers of nylon 6. We are particularly interested in the *onset* of chain folding as the oligoamides increase in length past the value of 6 nm, a common thickness in adjacent re-entry chain-folded nylon lamellae. In addition, the formation of once-folded, twice-folded, etc. chains is expected to introduce new structures amenable for analysis using diffraction physics and electron microscopy.

Nylon 6 Polymer Structures. Fibers. Three types of crystal structure have been reported for drawn fibers of nylon 6 polymer; referred to as an α-phase,[14] a less-stable β-phase,[14] and a γ-phase,[15−17] respectively. The salient features of the α-phase[14] structure are illustrated in Figure 1. Linear hydrogen bonds form between apolar chains to give hydrogen-bonded sheets in the *ac*-plane (Figure 1a). These sheets stack, via van der Waals interactions, with alternating shear parallel to the *c*-axis (Figure 1b) and progressive shear parallel to the *a*-axis (Figure 1c). This structure gives two interchain diffraction signals, characteristic of nylons, at spacings of 0.44 nm (200) and 0.37 nm (020/220), respectively. The single sheet, or even a single chain (see γ-phase structure of the 9-amide oligoamide later), generates a 002 diffraction signal from the planes of C═O groups at a spacing of 0.862 nm (see Figure 1a); the intensity of this signal will be a function of the relative magnitude of the *c*-axis shear between adjacent sheets in the two-sheet monoclinic unit cell (see Figure 1b,c). In the β-phase, the register of the sheets is different, less stable and the structure will convert into the α-phase.[14]

The characteristic features of the γ-phase are (1) a near-hexagonal unit cell with the two interchain distances closer together and in the region of 0.40−0.42 nm and (2) a chain (*c* -axis) repeat value reduced by ≈0.04 nm,[15] per amide unit, compared with the all-trans conformation. Various interpretations of the γ-phase in nylons have been reported,[15−18,8] with two issues of difference: (1) whether the hydrogen bonding occurs between neighboring polar, rather than apolar chains, and (2) whether the hydrogen bonds occur in one or more of the generalized interchain directions within the crystal.

Chain-Folded Lamellae. In studies on chain-folded nylon 6 crystals, prepared by refluxing the polymer in glycerine and cooling, Geil[19] reported two types of crystal morphology: (1) lozenge-shaped individual lamellae which gave two *hk*0 electron diffraction signals at spacings of 0.40 and 0.41 nm, which we judge resembles the γ-phase, and (2) ribbon-like lamellar in the form of

* To whom correspondence should be addressed. Telephone: +44(0)1179 288729 or 288733. Fax: +44(0) 1179 255624. E-mail: e.atkins@bristol.ac.uk.

S0024-9297(98)00519-1 CCC: $15.00
Published on Web 07/09/1998

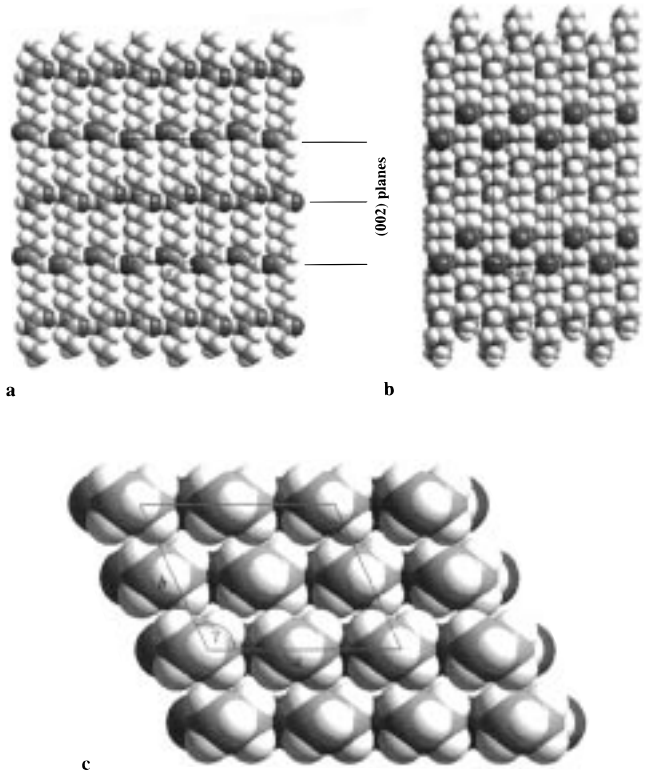

Figure 1. Three views of the α-phase structure of nylon 6 using the 5-amide oligoamide as the example. The monoclinic unit cell parameters: $a = 0.970$ nm, $b = 0.805$ nm, c (chain axis) $= 1.724$ nm, and $\gamma = 114°$ are close to those reported[14] for drawn fibers of the α-phase nylon 6 polymer, namely, $a = 0.956$ nm, $b = 0.801$ nm, c (chain axis) $= 1.724$ nm, and $\gamma = 115°$. Color code: white, hydrogen; light gray, carbon; dark gray, nitrogen; black, oxygen.

elementary spherulites which gave powder-like electron diffraction rings at spacings of 0.44 and 0.37 nm, values typical of the α-phase. In both cases, it was suggested[19] that the direction of the chains was orthogonal to the lamellar surface. Geil[19] noticed that the lozenge-shaped crystal exhibited sectorization and estimated the lamellar thickness to be in the range 5−10 nm. In 1963, Ogawa et al.[20] obtained higher resolution electron diffraction data from similar lamellar crystals of nylon 6 and confirmed that the lozenge-shaped crystals were indeed composed of the γ-phase structure. They also fractured the crystals on the substrate and showed the predominant fold direction was parallel to the long axis of the lozenge. The nature of the fold was not discussed in either of these papers.

Previous Studies on Monodisperse Oligoamides. Zahn[21] reported on the behavior in nylon 6 lamellar crystals from oligoamides of the type: $C_6H_5CH_2OOC-[NH(CH_2)_5CO]_nOH$, with n in the range of 1 to 12, i.e., each with a bulky aromatic unit at one end and a carboxylic acid group at the other end. Using low angle X-ray diffraction, he measured the lamellar stacking periodicity (LSP) from sedimented mats of lamellae and found a linear correlation with increasing chain length until the octomer (length ≈8 nm), beyond which the value of LSP remained constant. Further experiments by Zahn and Pieper[22] established that, above the octomer, the LSP values were dependent on solvent and crystallization conditions, while for the octomer and below the LSP values were solvent independent. Balta Calleja[23] and Keller[24] undertook additional X-ray experiments, both wide- and low-angle, together with electron microscopy, both imaging and diffraction, of lamellar crystals. Although the interpretation of the results[24] were clouded by concerns of chain obliquity to the lamellar normal, especially up to the higher oligomers, it was concluded that the chains remained straight (unfolded) up to ≈8 nm, beyond which chain-folding offered the most probable explanation.

Our Monodisperse Nylon 6 Oligoamides. We are studying the molecular organization, structure, and morphology of a series of lamellar-like crystals of monodisperse nylon oligomers using electron microscopy, both diffraction and imaging, together with X-ray diffraction. In this particular contribution we present our results on the 5-amide, 9-amide, and 17-amide oligomers of nylon 6 crystallized from trifluoroethanol and/or ethanol (the solvent) and 1,4-dioxane (miscible nonsolvent) mixtures. The molecules, or polymer chain segments, have lengths in the range 4.6−15 nm and the evidence will confirm that under our crystallization conditions they start to fold at the 9-amide oligomers (>8 nm). The molecules are terminated at the amine end by $-(CH_2)_2CH_3$ and at the carbonyl end by $-CH_2-CH_3$; thus, we expect no serious stereochemical problems with end groups. It should be noted that our results emanate from particular crystallization conditions; we could anticipate different structures and morphologies under different conditions.

Experimental Section

Materials. The starting materials, in the from of purified powders, were kindly provided by Drs. G. Brooke and S. Mohammed, University of Durham, Durham, U.K. The chemical synthesis and detailed characterization of these monodisperse oligoamides has already been reported by Brooke *et al.*[11,12]

Crystal Preparation. Choice of Crystallization Conditions. In polymeric materials, the crystallization process is only marginally affected by the bulk concentration of the polymeric solution, and the low solubility of the polymeric material in many solvents at room temperature means that the crystallization of polymers is usually achieved using elevated temperatures. The oligoamides, however, in particular the shorter chain materials, are more soluble, and the nucleation rate will be strongly concentration dependent. We can achieve a slow, controlled crystallization by the gradual evaporation of the solvent. Alternatively, we can induce a rapid nucleation rate by adding excess nonsolvent to the oligoamide solution; although the ensueing crystallization will be less controlled, this has the advantage that metastable crystalline forms are more likely to be trapped or "quenched-in". Thus in the oligoamide materials, we can achieve a range of different crystallization conditions at room temperature, allowing us to access the range of crystal forms available to the oligoamide material.

Crystallization Conditions. Each oligoamide material was crystallized from the same solvents using two different sets of conditions. (1) Fast crystallization: excess, filtered 1,4-dioxane (nonsolvent) was added to a filtered solution of the oligoamides in trifuoroethanol and/or ethanol. The solutions became turbid either immediately, or within a few minutes, once the excess nonsolvent had been added. (2) Slower crystallization: small quantities of 1,4-dioxane were added to undersaturated solutions of the oligoamides in excess trifluoroethanol and/or ethanol. After filtration, the trifluoroethanol and/or ethanol evaporation rate at room-temperature governed the crystallization rate.

Transmission Electron Microscopy. Samples for transmission electron microscopy (TEM) were prepared by depositing drops of the crystal suspension in 1,4-dioxane onto carbon-coated grids and allowing the 1,4-dioxane to evaporate over a few hours. The samples were examined at room temperature in both imaging and diffraction modes using a Phillips 400T

TEM operating at 100 kV. Some crystals were decorated with platinum/palladium to calibrate the diffraction patterns and to shadow the images.

X-ray Diffraction. X-ray diffraction patterns were obtained from sedimented mats of the oligoamide crystals. These mats were prepared by filtering the crystal suspensions using a glass syringe onto a 0.2 μm filter contained in a steel filter holder. The filter holder was then attached to a compressed air line to compact the crystals. X-ray diffraction patterns were obtained by directing a point-collimated beam parallel to the surface of the sedimented mats. The patterns were obtained at room temperature using a nickel-filtered Cu Kα radiation of length 0.1542 nm from a Phillips sealed beam X-ray generator operating at 35 kV and 40 mA. The wide-angle X-ray diffraction patterns were recorded on film, using an evacuated flat plate camera. Calcite ($d_B = 0.3035$ nm) was dusted onto selected samples for calibration purposes. The low-angle diffraction patterns were recorded on film at room temperature using a slit-collimated Rigaku-Denki camera and an Elliot GX-21 rotating target X-ray generator.

Computational Modeling. The software package Cerius 2, version 3.0 (Biosym/Molecular Simulations Inc.), was used in the structural modeling.

Results

5-Amide Nylon 6 Oligomer. Electron Microscopy: Imaging. A typical morphology for the 5-amide oligomer crystals is shown in Figure 2a. The crystals are ribbon-like (very long and thin) under our fast and slow crystallization conditions. Striations running along the length of the ribbons may be seen in many cases; some of the ribbons are also bent at fairly sharp angles.

Electron Diffraction. Many of the electron diffraction patterns of the 5-amide oligomer were obtained from twinned crystals (Figure 3a). Electron diffraction patterns of untwinned crystals were similar to patterns obtained from the polymeric material in the α-structure. There are a set of three prominent diffraction signal pairs, the inner pair at a spacing of 0.44 nm and the outer two pairs at a spacing of 0.37 nm. In the twinned crystals, the twinning occurs about the (020) composition plane. This is not unexpected, there are only weaker van der Waals forces in the [020] direction, and the energy difference between the sheets shearing by ≈ -0.17 nm in the *a*-direction (corresponding to a γ angle of 114°) or by sheets shearing $\approx +0.17$ nm (corresponding to a γ angle of 66°) will be relatively small. All the signals observed in the electron diffraction patterns are listed in Table 1.

X-ray Diffraction. The wide-angle X-ray diffraction pattern from sedimented mats of the 5-amide oligomer, taken with the X-ray beam orthogonal to the mat normal and mat normal vertical, is shown in Figure 4a. The diffraction signals (Table 1) index on a monoclinic unit cell with the following parameters: $a = 0.970$ nm, $b = 0.805$ nm, c (chain axis) $= 1.724$ nm, and $\gamma = 114°$. These unit cell parameters are close to those reported for the α-phase structure from drawn fibers of the nylon 6 polymer.[14] A comparison is given in Table 1. The two characteristic interchain diffraction signals occur on the equator at spacings of 0.44 nm (200) and 0.37 nm (020/$\bar{2}$20), respectively, in agreement with the electron diffraction data. The inner 0.44 nm signal is sharper than the outer 0.37 nm signal, indicating the difference between the relative precision of the interchain distances controlled by hydrogen bonds (*a*-direction) and the van der Waals forces (intersheet or *b*-direction).[3,5,7,13] A broad and relatively weak 002 diffraction signal occurs on the meridian at a spacing of 0.86 nm. We also observe the third and fourth orders of the lamellar stacking periodicity (LSP) on the meridian at spacings of 1.60 and 1.20 nm, respectively. The low-angle X-ray diffraction pattern (Figure 4a inset), shows a set of at least four orders of the LSP at 4.79 ± 0.01 nm.

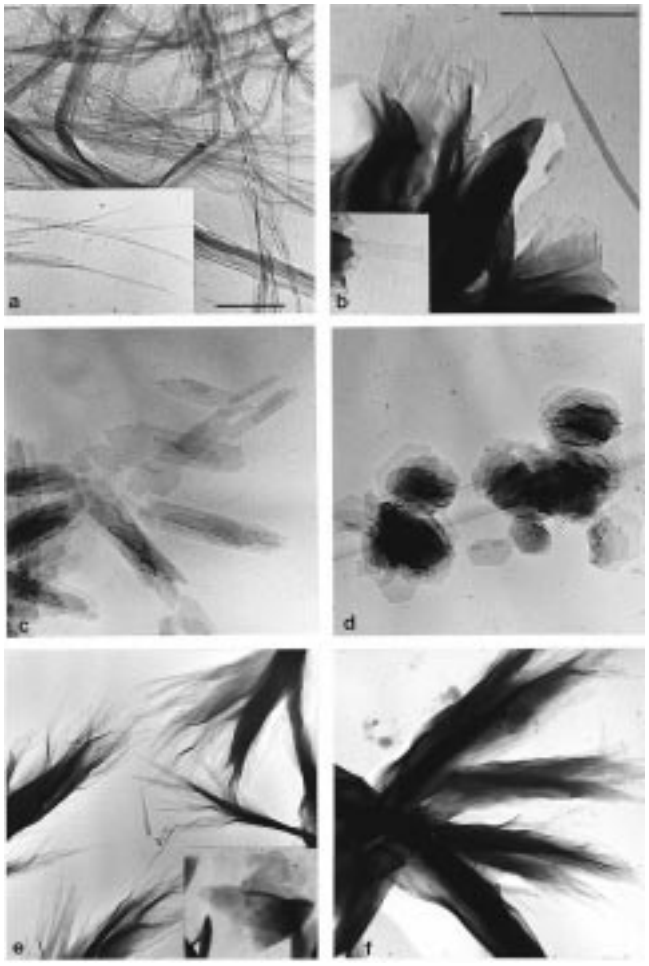

Figure 2. Transmission electron micrographs showing a number of lamellar crystalline morphologies obtained from the monodisperse nylon 6 oligoamides. The details of the crystallization conditions are given in the Experimental Section. Each scale bar represents 1 μm; parts c–f are to the same magnification as part a. (a) Ribbon-like crystals obtained on fast crystallization of the 5-amide oligomer. (b) Lathe-shaped lamellae obtained on rapid crystallization of the 9-amide oligomer. Note the specific angles occurring at the tips of these crystals. (c) Lazenge-shaped lamellae obtained on slower crystallization of the 9-amide oligomer. (d) A group of approximately hexagonal-shaped lamellae obtained from the slower crystallized 9-amide oligoamide. (e) Groups of lamellae obtained on rapid crystallization of the 17-amide oligomer. The ribbonlike lamellae can be seen to twist about their long axes (*a*-direction); the inset shows some crystals with a lower aspect ratio obtained on slower crystallization. (f) A typical group of chain-folded lamellae of polydisperse nylon 6 polymer. They are similar to the lamellae of the 17-amide oligomide shown in part e. These polymeric chain-folded lamellar crystals were obtained after thermal crystallization from 1,4-butanediol (seeding temperature 190 °C; crystallization temperature 115 °C[30] (electron micrograph courtesy of Dr. N. A. Jones). The crystals shown in parts a, b, e, and f have been shadowed with platinum/palladium.

9-Amide Nylon 6 Oligomer. Electron Microscopy: Imaging. The 9-amide oligomer crystals were lathlike and often multilayered and aggregated when crystallized under our rapid conditions (Figure 2b). Individual lamellae can be seen emanating outward from the multilayered aggregates, and these single

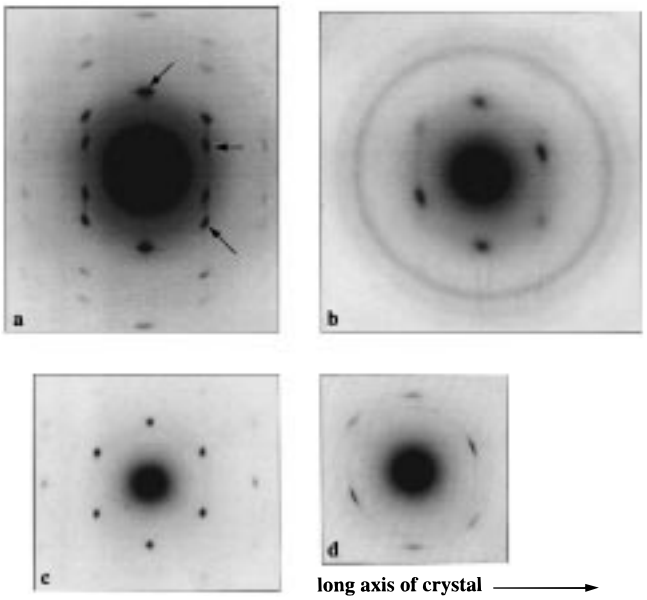

Figure 3. Electron diffraction patterns obtained from the nylon 6 oligoamide crystals with the electron beam orthogonal to the lamellae surfaces. (a) 5-Amide oligomer twinned crystal obtained under our fast crystallization conditions. The arrowed signals indicate the prominent diffraction signals that are observed for an untwinned crystal. (b) 9-Amide oligomer crystal obtained under our fast crystallization conditions. (c) 9-Amide oligomer crystal obtained under our slow crystallization conditions. (d) 17-Amide nylon 6 crystal obtained under our slow crystallization conditions. The diffraction signals are arced, indicating that the pattern was obtained from lamallae aggregates. Note the 100 diffraction signal is sharper and more intense than the outer two diffraction signals. All the patterns are to the same scale, and in (b) there is a Pt/Pd calibration ring.

crystals are often faceted; the angle between the faceted faces is close to the angle γ. Twinning often occurs in these crystals, and a number of microscopically twinned crystals are evident in Figure 2b. Striations running along the length of the crystals are also apparent in many cases; a number of the single crystals have serrated edges along their breadth. In contrast, the more slowly crystallized 9-amide oligomer crystals have a different morphology, as shown in parts c and d of Figure 2. The crystals are typically lozenge-shaped, often with coarsely serrated edges along their breadth. A few crystals also have a distinct hexagonal morphology (Figure 2d); the angle between the faces was measured to be $120 \pm 2°$.

Electron Diffraction. The electron diffraction pattern of the rapidly crystallized 9-amide nylon 6 oligomer, shown in Figure 3b, is similar to patterns obtained from the polymeric material. There are a set of three prominent diffraction signal pairs, one pair at a spacing of 0.44 nm and the other two pairs at a spacing of 0.37 nm (Table 2). Slower crystallized 9-amide oligomer crystals produced a different electron pattern as shown in Figure 3c and Table 3. This diffraction pattern is close to hexagonal, and the three prominent diffraction signal pairs have equal intensity and degree of sharpness. The spacings of these three diffraction signal pairs varied between 0.39 and 0.42 nm for different single crystals; the crystals with the (nearly) hexagonal morphology had the three spacings closer together (between 0.40 and 0.41 nm), while other more lozenge-shaped crystals had two inner signals at 0.42 nm and one outer signal at 0.39 nm.

X-ray Diffraction. The wide-angle X-ray diffraction pattern from sedimented mats from rapidly crystallized 9-amide oligomer is shown in Figure 4b. The diffraction signals (Table 2) index on a monoclinic unit cell with the following parameters: $a = 0.965$ nm, $b = 0.815$ nm, c (chain axis) $= 1.724$ nm, and $\gamma = 114°$, corresponding to the nylon 6 α-phase.[14] The two characteristic interchain diffraction signals occur on the equator at spacings of 0.44 nm (200) and 0.37 nm ($020/\bar{2}20$), respectively, in agreement with the electron diffraction data. As already described for the 5-amide oligomer, the 200 is sharper than the 020. A relatively weak 002 diffraction signal occurs on the meridian at a spacing of 0.86 nm. The low-angle X-ray diffraction pattern (Figure 4b inset) shows a strong, single LSP meridional peak at 4.60 ± 0.01 nm.

The wide-angle X-ray diffraction pattern from sedimented mats from slowly crystallized 9-amide oligomer is different (Figure 4c**),** and the diffraction signals index on a unit cell with parameters: $a = 0.492$ nm, $b = 0.465$ nm, $c = 1.672$ nm, $\alpha = \beta = 90°$, $\gamma = 122°$. The two characteristic interchain diffraction signals ($100/\bar{1}10$ and 010) on the equator are closer together, at spacings of 0.42 and 0.39 nm, respectively (see Table 3), in agreement with the electron diffraction data. There is a very strong 002 meridional diffraction signal at 0.84 nm. These diffraction features correspond to the nylon 6 γ-phase structure (see Introduction). In addition, a series of other diffraction signals occur on the meridian which can be separated into two categories. (1) A set of limited-lattice subsidiary maxima, associated with the 002, are observed. They turn out to be an array of seven between the origin and the 002 and emanate from a limited stack of nine 002 planes. The 4th, 5th, 6th, and 7th are visible together with the first few of the next just beyond the 002 at higher diffraction angles. These subsidiary maxima (Figure 4c) do not index on a Bragg lattice since they obey a different diffraction formula,[6,25] and we have checked that their positions conform to this formula.[25] (2) An extra meridional diffraction signal, at a spacing of 1.99 nm, and with a relative intensity noticeably stronger than the set of subsidiary maxima, is the fourth order of the LSP periodicity; this is confirmed by the observation in the low-angle X-ray pattern (Figure 4c inset) of the first four orders of a LSP of 7.97 ± 0.01 nm.

17-Amide Nylon 6 Oligomer. Electron Microscopy: Imaging. The rapidly crystallized 17-amide oligomer crystals consisted of multilayered aggregates (Figure 2e). Individual lamellae can be seen at the aggregate edges; some of these lamellae are twisting about their long axis (*a*-direction). This texture represents the initial stages of spherulitic growth. Under slower crystallization conditions, see Figure 2e inset, the crystals have a more "petal-like" morphology, and no twisting is evident. The morphology of the rapidly crystallized 17-amide oligomer resembles the morphology of the nylon 6 polymeric material grown from 1,4-butanediol at elevated temperatures (Figure 2f).

Electron Diffraction. The electron diffraction pattern of the rapidly crystallized 17-amide oligomer gave arced signals with spacings similar to those obtained from the α-phase polymeric material; the slower crystallized material gave less-arced patterns as shown in Figure 3d. The patterns have a set of three prominent diffraction signal pairs: one pair at spacing 0.44 nm and two at spacing 0.37 nm (Table 4). The inner 0.44 nm

Table 1. 5-Amide Nylon 6 Oligomer

electron diffraction spacings (nm) ±0.003 nm	estimated relative intensity	X-ray diffraction spacings (nm) ±0.01 nm (LSP) ±0.003 nm (WA)	orientation in X-ray pattern	estimated relative intensity	index	calculated spacing (nm)[a]
		4.79	M	s	LSP 001	4.791
		2.40	M	m	LSP 002	2.396
		1.597	M	m	LSP 003[b]	1.597
		1.197	M	w	LSP 004[b]	1.198
		0.864	M broad	vw	002	0.862
0.443	vs	0.443	E	vs	200	0.443
0.369	s	0.366	E broad	s	020	0.368
0.366	s	0.366	E broad	s	$\bar{2}20$	0.365
0.240	w				220	0.239
0.235	w				$\bar{4}20$	0.237
0.221	w				400	0.222
0.200	w				$\bar{2}40$	0.201
0.185	w				040	0.184
0.183	w				$\bar{4}40$	0.183

[a] Based on a monoclinic unit cell with the following parameters: $a = 0.970$ nm, $b = 0.805$ nm, $c = 1.724$ nm, $\alpha = \beta = 90°$, $\gamma = 114°$. The unit cell for nylon 6 polymer[14] is as follows: $a = 0.956$ nm, $b = 0.801$ nm, $c = 1.724$ nm, $\alpha = \beta = 90°$, and $\gamma = 112.5°$. [b] Also seen in the wide-angle X-ray pattern. WA = wide-angle X-ray diffraction. E = equator; Off-E = off equatorial; M = meridional; vs = very strong; s = strong; m = medium; w = weak; vw = very weak. *Note.* We also observe a medium-weak, broad off-meridional diffraction signal at 0.591 nm. We believe this signal emanates from a similar origin to the 0.561 nm (012) off-meridional signal reported for nylon 6 fibers[14](all the C=O groups lie close to these planes). In the 5-amide oligomer, the in-register stacking in the *c*-direction (as demonstrated by the fact that four orders of the LSP diffraction signals are seen and the fact that the lamellae intermesh to give a first-order LSP of value 4.79 nm), moves the sampling point to a spacing of 0.591 nm; thus, it can no longer be indexed on the unit cell subcell with parameters as above, but it now can be indexed as the (015) (calculated 0.584 nm) on the superlattice unit cell with the parameters $a = 0.970$ nm, $b = 0.805$ nm, $c = 4.79$ nm, $\alpha = \beta = 90°$, $\gamma = 114°$, which contain the whole of the 5-amide oligomer molecule.

signal is noticeably sharper and more intense than the outer two diffraction signals, indicative of the relative strengths of the intermolecular forces in the intrasheet and intersheet directions, respectively.

X-Ray Diffraction. The wide-angle X-ray diffraction pattern from sedimented mats from the fast-crystallized 17-amide oligomer is shown in Figure 4d. The diffraction signals (Table 4) index on a monoclinic unit cell with the following parameters: $a = 0.965$ nm, $b = 0.810$ nm, c (chain axis) $= 1.724$ nm, and $\gamma = 113°$, again corresponding to the nylon 6 α-phase structure.[14] The two characteristic interchain diffraction signals occur on the equator at spacings of 0.44 nm (200) and 0.37 nm (020/$\bar{2}$20), respectively; however, the 0.37 nm signal also has additional intensity deposited onto the meridian (Figure 4d). This arises because the 17-amide crystals twist about their long axis (*a*-direction), so that the 020 diffraction signal (orthogonal to the *a*-axis) will have intensity directed onto the meridian. Similarly, some intensity from the 0.44 nm (200) diffraction signal will be directed off the equator, also because of this twisting (the angle between *a* and *a** is 23°). As already described for the 5-amide oligomer, the 200 diffraction signal is sharper than the 020 signal. A relatively weak 002 diffraction signal occurs on the meridian at a spacing of 0.86 nm. The low-angle X-ray diffraction pattern (Figure 4d inset), shows a relatively strong, single meridional LSP peak at 5.36 ± 0.01 nm.

Discussion

We will first review the structures of the three oligoamide crystals, which are summarized in Table 5.

5-Amide Nylon 6 Oligoamide Structure. The diffraction data from this oligoamide are straightforward to interpret. The structure, shown in Figure 1, is essentially the same as the established α-phase structure of nylon 6[14] (parameter variations within 1.5%), except, of course, that it has a precise limit in the chain direction defining the lamellar thickness. However, we do have some extra features to discuss. The molecules are orthogonal to the lamellar surfaces, and the full length of the molecule is 4.61 nm; however, because of the alternating shear of the molecules, especially between the sheets, as illustrated in Figure 1b, the separation between the outer limits of the lamella thickness is 4.99 nm which exceeds the LSP spacing by 0.2 nm, or 4%. In other words, there is intedigitation of adjacent lamella by this amount *on average*. The grooves in the lamellar surfaces are at least 0.33 nm deep (see Figure 1b), and so the average penetration value of 0.2 nm is stereochemically possible. Although the LSP diffraction signals are reasonably sharp, indicating a respectable correlation length in the lamellar stacking direction, their intensity falls to below threshold after the fourth order, indicating fluctuations in the stacking periodicity; thus, the value of 0.2 nm is an average figure. The precise interdigitation might be frustrated by the extra bulkiness or rotation of the terminal methyl groups.

With only five 002 planes within each lamella, the possibility of limited lattice subsidiary maxima needs to be considered.[25] Unfortunately, for this particular case, they are not observed owing to the relative *c*-axis shear between successive pairs of sheets within the unit cell. This reduces the intensity of the 002 and lowers the intensity of the subsidiary maxima below the background noise level. The relative line width of the 002 diffraction signal, however, is commensurate with five repeats.

9-Amide Nylon 6 Oligoamide Structures. This monodispersed oligoamide gave two quite different X-ray diffraction fingerprints depending on the rate of crystallization.

The Onset of Folding: Rapidly Crystallized α-Phase Structure. The analysis of the wide-angle X-ray diffraction pattern, supplemented with the electron diffraction data, establishes the usual α-phase structure,[14] and (*importantly*) the chain direction is confirmed to be orthogonal to the lamellar surface; i.e., the lamellar core is similar to the structure shown in Figure 1 for the 5-amide oligomer. However, we hasten to add that the strong low-angle diffraction signal, which

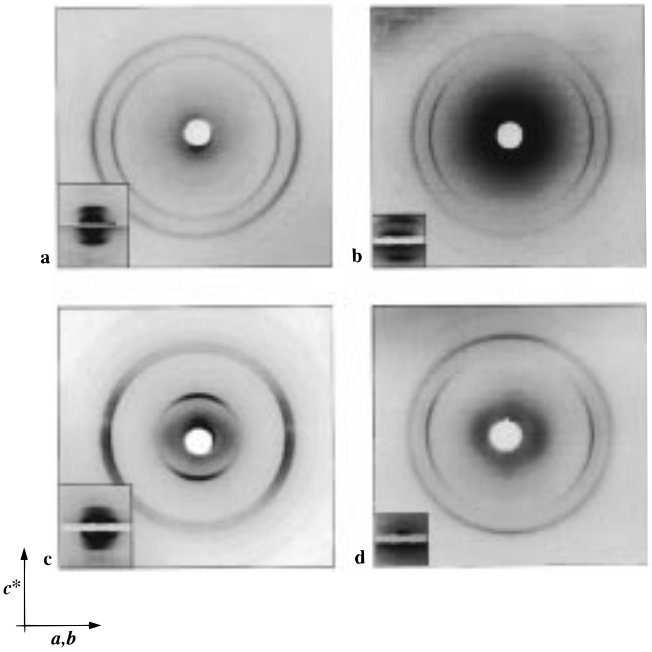

Figure 4. X-ray diffraction patterns from sedimented mats; beam parallel to the mat surface and the mat normal vertical. The low-angle signal is shown as an inset in the lower left corner of each wide-angle diffraction pattern. (a) 5-Amide oligomer. (b) 9-Amide oligomer crystals grown under our fast crystallization method. (c) 9-Amide oligomer crystals grown under our slow crystallization method. (d) 17-Amide oligomer crystals grown under our fast crystallization method. The patterns are to the same scale. Note that in parts a, b, and d there are two prominent interchain diffraction signals: an inner equatorial diffraction signal at spacing 0.44 nm and an outer, broader signal at 0.37 nm. The signal at 0.37 nm is equatorial in parts a and b, but in part d this signal has additional intensity deposited onto the meridian. This is a consequence of the fast-crystallized 17-Amide lamellae twisting about the *a*-axis (see Figure 2e). These diffraction signals at 0.44 and 0.37 nm are characteristic of the nylon 6 α-phase crystal structure.[14] In part c, the two prominent interchain diffraction signals are spaced closer together (at 0.42 and 0.39 nm, respectively) and there is also an intense meridional signal. These diffraction signals are typical of the nylon 6 γ-phase[15] rather than the α-phase structure. A weak equatorial diffraction arc is noticed in parts a and b at a spacing of 0.42 nm. We associate this with a minor component of the γ-phase.[6] The outer continuous ring (just inside the box) in parts a, b, and d is a calcite calibration ring.

we know to be the first and only order and to be at a spacing of 4.60 ± 0.01 nm, is almost half the length, 8.06 nm, of the 9-amide, all-trans conformation. Thus, the chains *must be once-folded*, and they run *orthogonal* to the lamellar surface and crystallize in the α-phase structure. Under the conditions of crystallization used, we have established, without doubt, the onset of folding in these monodisperse oligoamides. It is perhaps worth mentioning at this point, that chain-folded lamellar crystals usually only show a single, first-order LSP diffraction signal, and without annealing to improve the stacking, LSP values of up to 0.5 nm larger than the lamellar thickness are found.[26]

The Nature of Once-Folded Chains in a Lamella. On first thoughts, taking into account the need to satisfy the interchain hydrogen bonds, one envisions a simple hairpin conformation, as illustrated in Figure 5a. This once-folded molecule has a length of 4.09 nm and therefore could be accommodated within the measured LSP distance of 4.60 ± 0.01 nm. There are two aspects of this once-folded conformation that deserve comment.

(1) The fold contains an amide unit, a direct consequence of the odd number of amide units in the molecule. To our knowledge, there is no published literature discussing the nature of the fold in nylon 6 chain-folded lamellar crystals. It is probably fair to say that until an amide fold geometry was established by Atkins *et al.*[1] in 1992 for the nylon 4 6 chain-folded lamellar, it was assumed that the folds in nylon 6 consisted of alkane segments. This is not the case for all nylons, since for short alkane segments, e.g. nylon 4[27] and polypeptides[28] (nylon 2 backbone), the folds must contain *at least* one amide unit. In the case of chain-folded lamellar crystals of $2N$ $(N + 1)$ nylons, viz. 4 6, 6 8, 8 10, and 10 12, Jones *et al.*[7] discovered that nylons 4 6 and 6 8 had amide units in the folds and hydrogen-bonded sheets similar (alternating shear), but certainly not identical, to nylon 6. However, the nylon 8 10 and nylon 10 12 crystals had alkane segment folds and hydrogen-bonded sheets with progressive shear. Indeed, the nature of the fold (amide or alkane) was coupled to the type of hydrogen-bonded sheet structure, and therefore it was argued that the preferred sheet structure (and possibly its packing) was influenced by the type of fold. For nylon 6 this is not the case, since it is a polar molecule and it does not matter whether the fold is alkane or amide; the hydrogen-bonded sheet structure is invariant. Of course, it can be argued that placing an amide in the fold reduces the overall number of intrasheet hydrogen bonds; however, there are other elements to be considered relating to the interaction of the molecules with the solvent during crystallization (for discussion see ref 7).

(2) We need to inquire how the once-folded conformation shown in Figure 5a packs into the lamellar crystal. One possibility is shown in Figure 5c: all the folds decorate one lamellar surface; i.e., we have a polar crystal. After making allowance for the usual intersheet shear in the α-phase structure, the lamellar thickness to the outer boundaries is 4.46 nm, compared with the measured value of 4.60 ±0.01 nm. There is, however, another possible packing arrangement to consider, as illustrated in Figure 5d; the once-folded molecules pack with opposite polarity, and so both lamellar surfaces are equally populated with folds. In this case the outer-boundary lamellar thickness is 4.68 nm. Although this extreme value is slightly greater than the measured value, the structure can cope with some degree of interdigitation without any implications for the low-angle diffraction results; i.e., higher orders would not be generated. We judge it unlikely that the polar lamellar structure (Figure 5c) is an appropriate model; if such lamellae stacked with like surfaces together, bilamellar structures would form, contrary to the experimentally observed LSP values. Thus, the most plausible scenario is that once-folded molecules pack in a random "up and down" fashion within the lamellae (Figure 5d).

Finally, we need to consider the consequences if a 9-amide oligomer folded asymmetrically, i.e., with an alkane fold, even if only to eliminate such a conformation. This conformation is shown in Figure 5b. The maximum length is 4.46 nm, and the *only* plausible packing scheme is direct juxtapositioning of molecules with the folds decorating one lamellar surface; this is similar to the intermolecular arrangement illustrated in Figure 5c. After allowing for the α-phase intersheet

Table 2. 9-Amide Nylon 6 Oligomer: Rapid Crystallization[b]

electron diffraction spacings (nm) ±0.003 nm	estimated relative intensity	X-ray diffraction spacings (nm) ±0.01 nm (LSP) ±0.003 nm (WA)	orientation in X-ray pattern	estimated relative intensity	index	calculated spacing (nm)[a]
		4.60	M	s	LSP 001	4.60
		0.862	M broad	vw	002	0.862
0.440	s	0.443	E	s	200	0.441
0.374	m	0.371	E broad	s	020	0.372
0.369	m	0.371	E broad	s	$\bar{2}20$	0.367

[a] Based on a monoclinic unit cell with the following parameters: $a = 0.965$ nm, $b = 0.815$ nm, $c = 1.724$ nm, $\alpha = \beta = 90°$ and $\gamma = 114°$. A weak, diffuse off-meridional diffraction signal is observed which cannot be accounted for on the basis of this unit cell. We believe it indexes as the 014 of the LSP lattice, i.e., with $c = 4.60$ nm. [b] Symbol notation is the same as in Table 1.

Table 3. 9-Amide Nylon 6 Oligomer: Slower Crystallization[e]

electron diffraction spacings[d] (nm) ±0.003 nm	estimated relative intensity	X-ray diffraction spacings (nm) ±0.01 nm (LSP) ±0.003 nm (WA)	orientation in X-ray pattern	estimated relative intensity	index	calculated spacing (nm)[a]
		7.97	M	s	LSP 001	7.972
		3.99	M	m	LSP 002	3.986
		2.66	M	m	LSP 003	2.657
		1.993	M	m	LSP 004[b]	1.993
		0.836	M	vs	002[c]	0.836
		0.418	M	w	004	0.418
		0.279	M	w	006	0.279
		0.207	M	w	008	0.209
0.417	s	0.418	E	vs	$1\bar{0}0$	0.417
0.418	s	0.418	E	vs	$\bar{1}10$	0.418
0.395	s	0.390	E	vs	$0\bar{1}0$	0.394
0.247	w				$\bar{2}10$	0.246
0.231	w				$1\bar{1}0$	0.232
0.231	vw				$\bar{1}20$	0.232

[a] Based on a monoclinic unit cell with the following parameters: $a = 0.492$ nm, $b = 0.465$ nm, $c = 1.672$ nm, $\alpha = \beta = 90°$, and $\gamma = 122°$. [b] Also seen in the wide-angle X-ray pattern. [c] The last four members of an array of seven subsidiary maxima are observed inside (first few masked by beam stop) the 002 and also the first few members of the next tranche are seen beyond the 002. [d] Exact diffraction spacings vary slightly between different crystals. The spacings are closer to hexagonal for the more hexagonal-shaped crystals. [e] Symbol notation is the same as in Table 1.

Table 4. 17-Amide Nylon 6 Oligomer

electron diffraction spacings (nm) ±0.003 nm	estimated relative intensity	X-ray diffraction spacings (nm) ±0.01 nm (LSP) ±0.003 nm (WA)	orientation in X-ray pattern	estimated relative intensity	index	calculated spacing (nm)[a]
		5.36	M	vs	LSP 001	5.36
		0.857	M broad	vw	002	0.862
0.443	s	0.444	E	s	200	0.444
0.372	m	0.372	E broad[b]	s	020	0.373
0.363	w	0.372	E broad[b]	s	$\bar{2}20$	0.364

[a] Based on a monoclinic unit cell with the following parameters: $a = 0.965$ nm, $b = 0.810$ nm, $c = 1.724$ nm, $\alpha = \beta = 90°$, and $\gamma = 113°$. [b] This 0.372 nm signal has additional intensity directed onto the meridian due to the twisting of the 17-amide crystals about the *a*-axis.

Table 5. Summary of Crystallization Conditions and the Resulting Crystal Structures

nylon 6 oligomer	crystallization conditions	morphology	crystal phase	chain length (nm)	LSP (nm)	folding status
5-amide	rapid/slower crystallization	ribbon-like	nylon 6 α-phase	4.6	4.8	unfolded
9-amide	rapid crystallization	lathe-like	nylon 6 α-phase	8.0	4.8	once-folded
9-amide	slower crystallization	lozenge-shaped or hexagonal	nylon 6 γ-phase	7.8 (hex)	8.0	unfolded
17-amide	rapid/slower crystallization	lathe-like	nylon 6 α-phase	15.0	5.4	twice-folded

shear, the lamellar thickness, to the outer boundaries, is 4.83 nm. The amide units in each tail cannot form hydrogen bonds, even if bilamellae form, since the C_3H_7 end segments are too long for stereochemical interdigitation. The tail on the righthand side of the alkane-fold conformation (Figure 5b) could of course be bent around, as long as it stays within the *ac*-sheet. However, the outer-limit thickness would still be greater than the amide-fold hairpin conformation shown in Figure 5a. Thus, the structure shown in Figure 5d, which utilizes the Figure 5a amide-fold conformation, appears to be the better of the contenders.

Unfolded Structure: Slowly Crystallized γ-Phase. The analysis of the wide-angle X-ray pattern, supplemented with the electron diffraction data, shows that the γ-phase structure is formed on slow crystallization of the 9-amide oligomer and that the chain direction is orthogonal to the lamellar surface. In this form, the prominent interchain spacings have similar spacings in the range of 0.39 nm to 0.42 nm, and the lack of *c*-axis chain shear produces an intense meridional signal corresponding to the interamide spacing in the X-ray diffraction patterns (see Figure 4c, Table 3). The length of the unfolded 9-amide oligomer in a γ-phase conforma-

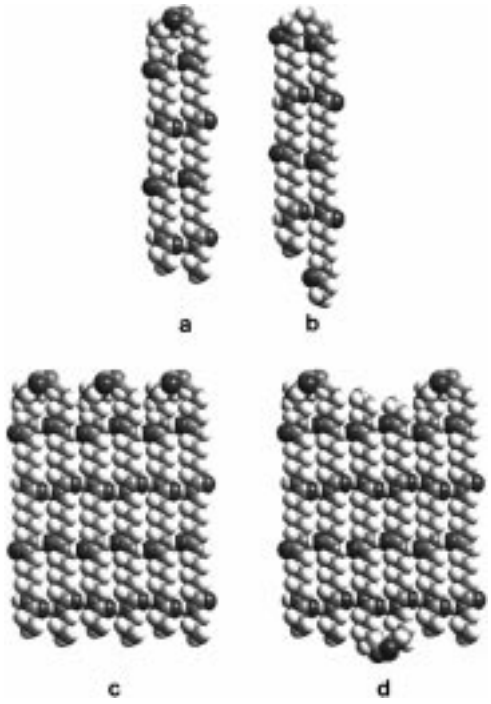

Figure 5. Possible fold conformations and their packing arrangements in the once-folded 9-amide nylon 6 oligomer crystals. The color code is as in Figure 1. (a) Once-folded 9-amide oligomer chain. The hairpin fold occurs at the chain midpoint and consequently, the fold contains an amide unit. (b) Once-folded 9-amide oligomer chain with the hairpin fold containing an alkane segment. This asymmetric folding arrangement can be discarded as a model for our once-folded 9-amide nylon 6 structure, since the LSP generated from the packing of these folded molecules would be too large in comparison with our experimental value. (c) Packing of the once-folded molecules shown in part a so that all the folds decorate the top surface of the hydrogen-bonded sheet, creating a polar structure. (d) Packing of the once-folded molecules shown in part a so that folds decorate both the top and bottom surfaces of the hydrogen-bonded sheets. We consider this the most likely packing mode of the once-folded chains.

tion is 7.78 nm (compared with 8.02 nm for an all-trans conformation). Since the chains in the γ-phase crystal have no *c*-axis shear, the γ-phase 9-amide oligoamide lamellae would also be 7.78 nm in thickness and can therefore pack within the measured LSP of 7.97 $\pm$0.01 nm. The appearance of the array of seven subsidiary maxima is overwhelming evidence for a crystalline lamella composed of unfolded chains, with nine strongly scattering planes.[25]

Evidence for Hydrogen Bonding in Three Directions. In this γ-phase, we believe the (near) hexagonal packing of the chains at interchain spacings typical of hydrogen-bonded chains suggests that hydrogen bonds are formed in three trigonal directions, but not in general with equal population,[29] in this crystal structure (see Figure 6). The morphology of the 9-amide oligomer unfolded γ-phase crystals fully supports this model (see Figure 2c, d) since the majority of the crystals are lozenge-shaped or have a hexagonal morphology, indicative of similar growth rates and hence similar intermolecular forces, in the three trigonal directions. The relative sharpness and intensity of the prominent interchain spacings in both the electron diffraction and X-ray diffraction patterns is also similar (Figures 3c and 4c), indicative of similar interchain forces.

In the nylon 6 γ-phase, the three directions of hydrogen bonding will necessarily be between chains

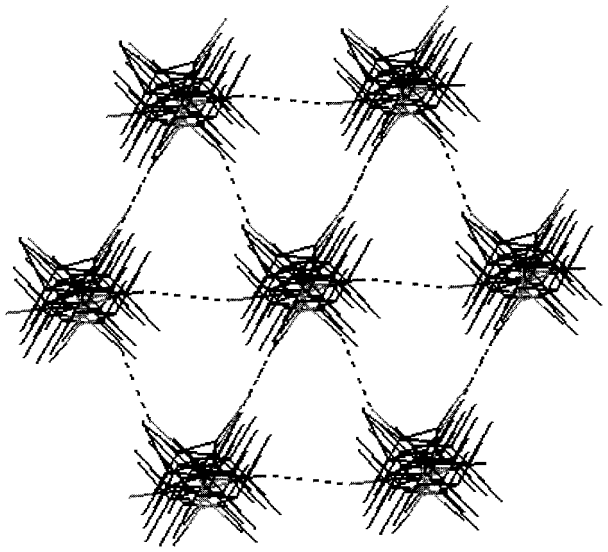

Figure 6. View parallel to the *c*-direction (chain axis) of the unfolded 9-amide nylon 6 γ-phase crystals showing the three trigonal directions of the hydrogen bonds proposed for this structure. It should be noted that we are not suggesting equal population of the hydrogen bonds in the three principle directions. Color code: methylene units are in black and amide groups in gray; hydrogen bonds are shown by dashed lines.

of opposite polarity in two directions and be between unidirectional chains in the other trigonal direction. In contrast, the γ-phase of the unfolded 9-amide oligomer can, in principle, have hydrogen bonds between all unidirectional chains; this form of hydrogen bonding is advantageous because the amide dipoles are aligned. However, if all the chains were unidirectional, we would expect a structure analogous to the form reported for the 3-amide nylon 6 oligomer,[13] i.e., one with progressive hydrogen bonding in two directions, since this structure would entail the least disruption to the lowest energy all-trans conformation of the chain backbone. Similarly, if every other chain were opposite in polarity, we might expect the α-phase nylon 6 hydrogen-bonded sheet structure to occur, since the fully trans conformation of the chain backbone is retained. Thus, we believe the unfolded γ-phase 9-amide oligomer consists of a random array of up and down chains. This model is supported by the fact that the unfolded γ-phase 9-amide oligomer did not convert to a more-stable room-temperature phase on annealing.

Onset of Folding in the 9-Amide Nylon 6 Oligomer. We can confirm that the onset of folding occurs in the 9-amide oligomer. The folding is induced by rapid crystallization from a *dilute* solution containing an excess of a *weaker* bonding solvent. These conditions favor chain-folding since the individual chains are likely to form hydrogen bonds within each molecule before they encounter another molecule to which they can hydrogen bond. If the crystallization rate is slowed, however, unfolded 9-amide oligomer crystals occur.

17-Amide Nylon 6 Oligoamide Structure. The analysis of the wide-angle X-ray pattern, supplemented with the electron diffraction data, establishes the usual α-phase structure.[14] The chain direction is orthogonal to the lamellar surface; i.e., the lamellar core is similar to the structure shown in Figure 1. The full length of the 17-amide molecule is 14.96 nm. The strong low-angle diffraction signal, which we know to be the first and only order, is at a spacing of 5.36 $\pm$ 0.01 nm. These results suggest that the chains are twice-folded. There

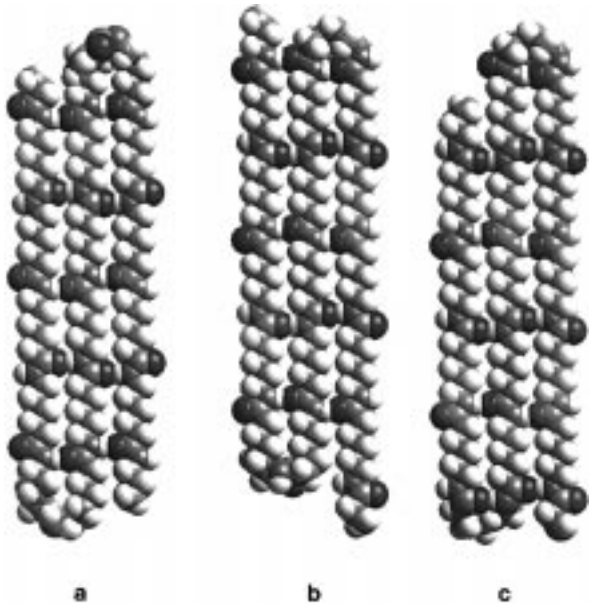

Figure 7. Possible fold conformations in the twice-folded 17-amide oligomer crystals. The color code is as in Figure 1. Key: (a) 17-amide oligomer containing two amide folds; (b) 17-amide oligomer containing one amide and one alkane fold; (c) 17-amide nylon 6 chain containing two alkane folds.

are three twice-folded conformations (see Figure 7) that have thicknesses close to the LSP of 5.36 nm: (1) a conformation with two amide folds as shown in Figure 7a, with a thickness of 5.17 nm; (2) a conformation with one amide fold and one alkane fold and thickness of 5.42 nm (Figure 7b); (3) a conformation with two alkane folds as shown in Figure 7c with a thickness of 5.30 nm. Solely on the basis of the thickness dimensions of an individual molecule, it is difficult to selectively delineate between the three models, except to note that model 2 is less favorable. The differences between the models increases when consideration is given to their association into hydrogen-bonded sheets and crystallization into the α-phase structure. It turns out, that for each of the three twice-folded molecules there is only one way each molecule can juxtapose to form the nylon 6-like hydrogen-bonded sheets. The three structures are shown in Figure 8, and in all cases contiguous molecules associate in an antiparallel fashion. Two features emerge: (i) the hydrogen-bonded sheet thickness for the amide/alkane fold conformation (model 2) increases to 5.55 nm; (ii) the surface roughness is different in each case. On both these features we judge that the model 2 conformation (Figure 8b) can be ruled out, leaving only models 1 and 3 to consider further. When allowance is made for the intersheet shear, the lamellar thickness becomes 5.54 and 5.67 nm for models 1 (Figure 8a) and 3 (Figure 8c), respectively. We will expect some interdigitation of the stacked lamellae, but the all-amide folded structure (model 1: Figure 8a) fits the data better. Allowing for both the α-phase intersheet shear and some interlamellar interdigitation, the lamellar thickness for model 1 reduces to 5.22 nm, a value commensurate with the experimental LSP value of 5.36 ±0.01 nm.

Morphology of the Oligoamide Crystals. If we crystallize the unfolded oligoamides by adding a nonsolvent that cannot hydrogen bond so effectively to the oligoamide, the fastest crystal growth direction(s) will tend to be the hydrogen bond direction(s). Consequently, under our crystallization conditions, the resulting crystal morphologies reflect the number of hydrogen bond directions. One hydrogen bond direction leads to long, narrow crystals; two hydrogen bond directions (or unequal population of three hydrogen bond directions) lead to wider crystals, while an equal population of three trigonal hydrogen bond directions produces crystals with a distinct hexagonal morphology. A similar correlation between the number of hydrogen bond directions and the resulting crystal morphology has been observed in our 3-amide nylon 6 and 3-amide nylon 6 6 crystals.[13]

In the folded crystals, however, the morphology is also influenced by the folding, which occurs principally in one direction. Hence, the link between the number of hydrogen bond directions and crystal shape is not so evident; the crystals tend to be individual lamellae (no in-register stacking in the direction of the lamellar normal), lath-like and multilayered, in particular when crystallized from a relatively concentrated solution.

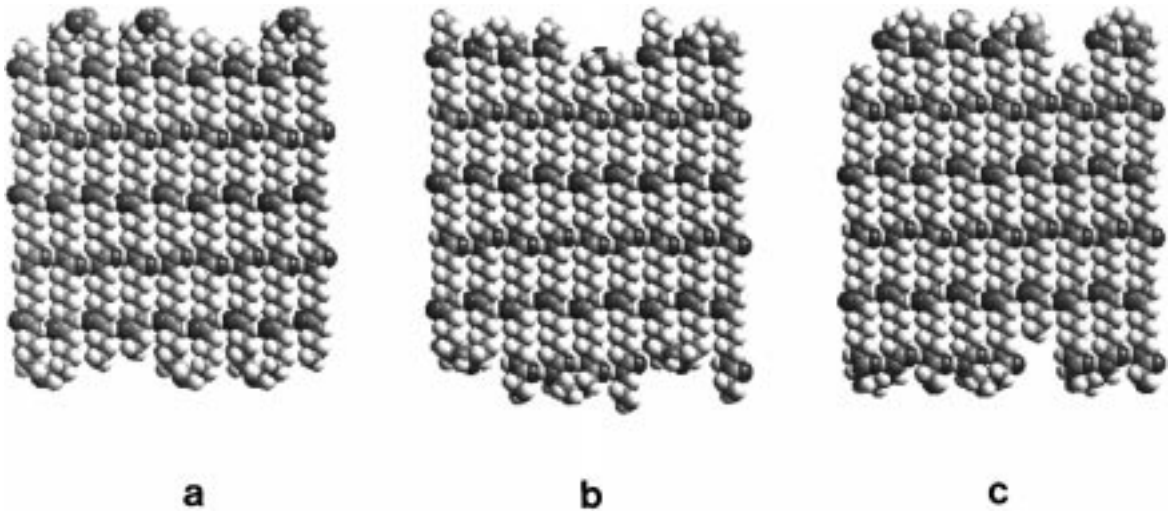

Figure 8. Possible chain packing arrangements of the hydrogen-bonded sheets in the twice-folded 17-amide oligomer crystals. In each case, adjacent molecules pack with opposite polarity. The color code is as in Figure 1. Key: (a) 17-amide oligomer containing two amide folds; (b) 17-amide oligomer containing one amide and one alkane fold; (c) 17-amide oligomer containing two alkane folds. In view of the experimental value obtained for the LSP, we believe model a represents the most likely fold conformation and packing mode of the 17-amide oligomer.

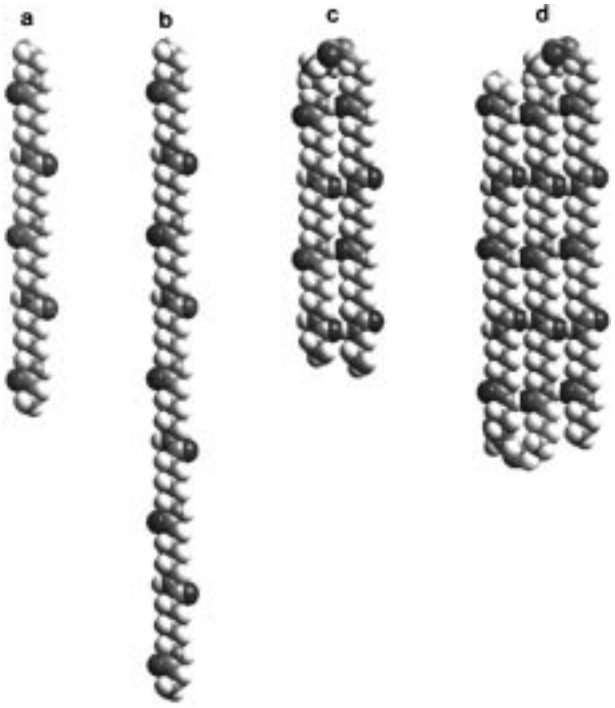

Figure 9. The four proposed conformations of the nylon 6 oligomers. Key: (a) unfolded 5-amide oligomer; (b) unfolded 9-amide oligomer; (c) once folded 9-amide oligomer; (d) twice-folded 17-amide oligomer. Note: the molecule as shown in part b is in the extended all-trans planar conformation. In the actual structure (γ-phase) the amide units rotate out of the plane and the length of the molecule shortens slightly.

Conclusions

Under the crystallization conditions used, the 5-, 9-, and 17-amide nylon 6 oligomers crystallize in the nylon 6 polymeric α-phase structure, i.e., hydrogen-bonded sheets stacking via van der Waals forces. In addition, the 9-amide oligomer also crystallized in a γ-phase structure. The experimental evidence supports a model (Figure 6) with interchain hydrogen bonding occurring in the three principle trigonal directions, but not with equal population, for this γ-phase structure. In unfolded oligoamide crystals, the crystal morphology is indicative of the number of hydrogen bond directions: one direction generates ribbon-like crystals, two directions (or three unequally populated directions) produce lozenge- or plate[13]-shaped crystals, and three equally populated directions induce crystals with hexagonal morphology. A degree of in-register stacking in the direction of the lamellar normal (c*-axis) is possible in both the unfolded 5-amide α-phase crystals and unfolded 9-amide γ-phase crystals.

The 5-amide oligomer remains unfolded (Figure 9a), irrespective of the rate of crystallization used. Under conditions of relatively slow crystallization the 9-amide oligomer also remains unfolded (Figure 9b) but crystallizes in a γ-phase structure. At relatively rapid crystallization rates, the 9-amide molecule crystallizes in the α-phase structure and folds in half; the preferred hairpin conformation has an amide in the fold (Figure 9c). Thus, in this series of nylon 6 oligomers, the onset of folding occurs when there are nine amide units in the chain.

The 17-amide oligomer forms a twice-folded conformation (Figure 9d), which crystallizes in the nylon 6 α-phase structure, and the evidence favors amide units in both folds. Figure 9 summarizes and illustrates the four different molecular conformations proposed. When we have the opportunity to examine the folding of longer nylon 6 oligomers in lamellar crystals, it will be of interest to see if the structures adopt amide folds or whether the folds occur in the alkane segments. Indeed, to our knowledge, the nature of the folds in chain-folded polymeric nylon 6 lamellae has yet to be established.

Acknowledgment. We are most grateful to Drs. G. Brooke and S. Mohammed for supplying pure, monodisperse oligoamide samples which made this study possible. We thank the Engineering and Physical Sciences Research Council, U.K., for financial support, including a postdoctoral fellowship to S.J.C.

References and Notes

(1) Atkins, E. D. T.; Hill, M. J.; Hong, S.; Keller, A.; Organ, S. J. *Macromolecules* **1992**, *25*, 917.
(2) Atkins, E. D. T.; Hill, M. J.; Veluraja, K. *Polymer* **1995**, *36*, 35.
(3) Hill, M. J.; Atkins, E. D. T. *Macromolecules* **1995**, *28*, 604.
(4) Jones, N. A.; Atkins, E. D. T.; Hill, M. J.; Cooper, S. J.; Franco, L. M*acromolecules* **1996**, *29*, 6011.
(5) Jones, N. A.; Atkins, E. D. T.; Hill, M. J.; Cooper, S. J.; Franco, L. *Polymer* **1997**, *38*, 2689.
(6) Jones, N. A.; Cooper, S. J.; Atkins, E. D. T.; Hill, M. J.; Franco, L. *J Polym. Sci., B* (*Polym. Phys.*) **1997**, *35*, 675.
(7) Jones, N. A.; Atkins, E. D. T.; Hill, M. J.; Cooper, S. J.; Franco, L. *Macromolecules* **1997**, *30*, 3569.
(8) Franco, L.; Cooper, S. J.; Atkins, E. D. T.; Hill, M. J.; Jones, N. A. *J Polym. Sci., B* (*Polym. Phys*) **1998**, *36*, 1153.
(9) Atkins, E. D. T.; Hill, M. J.; Jones, N. A.; Cooper, S. J. *J Polym. Sci., B* (*Polym. Phys.*) **1998**, in press.
(10) The chemical synthesis of these high-pedigree monodisperse oligoamides by Dr. G. Brooke and his colleagues at the Chemistry Department, University of Durham, was in response to a desire by Prof. E. Atkins and his colleagues at the Physics Department, University of Bristol, for high-fidelity oligo- and polyamides that are necessary for studying fundamental aspects of polymer physics: in this case, the suble interplay between van der Waals interactions, hydrogen bonding, chain-folding, and crystallization. We appreciate the foresight of the Engineering and Science Research Council, U.K., in supporting this collaborative venture.
(11) Brooke, G. M.; Mohammed, S.; Whiting, M. C. *Chem. Commun.* **1997**, *16*, 1511.
(12) Brooke, G. M.; Mohammed, S.; Whiting, M. C. *J. Chem. Soc., Perkin Trans. I* **1997**, *22*, 3371.
(13) Cooper, S. J.; Atkins, E. D. T.; Hill, M. J. Submitted to *J. Polym. Sci., B* (*Polym. Phys.*), in press.
(14) Holmes, D. R.; Bunn, C. W.; Smith, D. J. *J. Polym. Sci.* **1955**, *17*, 159.
(15) Kinoshita, Y. *Makromol. Chem.* **1959,** *33*, 1, 21.
(16) Vogelsong, D. C. *J. Polym. Sci. A* **1963,** *1*, 1055.
(17) Bradbury, E. M.; Brown, L.; Elliott, A.; Parry, D. A. D. *Polymer* **1965**, *6*, 465.
(18) Navarro, E.; Franco, L.; Subirana, J. A.; Puiggali, J. *Macromolecules* **1996,** *28*, 8742.
(19) Geil, P. H. *J. Polym. Sci.* **1960,** *44*, 449.
(20) Ogawa, M.; Ota, T.; Yoshizaki, O.; Nagai, E. *J. Polym. Sci., Polym. Lett.* **1963,** *1*, 57.
(21) Zahn, H. Presented at the International Symposium on Macromolecules, Wiesbaden, Germany, October, 1959.
(22) Zahn, H.; Pieper, E. W. *Kolloid Z.* **1962,** *180*, 97.
(23) Balta Calleja, F. J. Ph.D. Thesis, University of Bristol, U.K., 1962.
(24) Balta Calleja, F. J.; Keller, A. *J. Polym. Sci. A* **1964**, *2*, 2151.
(25) Atkins, E. D. T.; Keller, A.; Sadler, D. M. *J. Polym. Sci. A* **1972**, *2*, 863.
(26) Dreyfuss P.; Keller A. *J. Makromol. Sci. (Phys).* **1970**, *B4* (4), 811. Dreyfuss P.; Keller A. *J. Polym. Sci. 1970, B8, 253.*
(27) Bellinger, M. A.; Waddon, A. J.; Atkins, E. D. T.; MacKnight, W. J. *Macromolecules* **1994,** *27*, 2130.

(28) Krejchi, M. T.; Atkins, E. D. T.; Waddon, A.; Fournier, M. J.; Mason, T. L.; Tirrell, D. A. *Science* **1994**, *265*, 1427. Panitch, A.; Matsuki, K.; Cantor, E. J.; Cooper, S. J.; Atkins, E. D. T.; Fournier, M. J.; Mason, T. L.; Tirrell, D. A. *Macromolecules* **1997**, *30*, 42. Krejchi, M. T.; Cooper, S. J.; Deguchi, Y.; Atkins, E. D. T.; Fournier, M. J.; Mason, T. L.; Tirrell, D. A. *Macromolecules* **1997**, *30*, 5016. Cantor, E. J.; Atkins, E. D. T.; Cooper, S. J.; Fournier, M. J.; Mason, T. L.; Tirrell, D. A. *J. Biochemistry* **1997**, *122*, 2217.

(29) In the 9-amide nylon 6 γ-phase crystals, the interchain distances are between 0.465 and 0.492 nm; these values are typical of those expected for amide interchain hydrogen-bonded distances. The relative population of each of the trigonal hydrogen bond directions in the γ-phase will then depend on the relative strengths of the hydrogen bonds formed in each direction.

(30) Jones, N. A. Ph.D. Thesis, University of Bristol, U.K., 1996.

MA9805194